Experimental and theoretical assignment of the vibrational spectra of triazoles and benzotriazoles. Identification of IR marker bands and electric response properties

ARTICLE *in* JOURNAL OF MOLECULAR MODELING · MARCH 2014

Impact Factor: 1.74 · DOI: 10.1007/s00894-014-2078-y · Source: PubMed

5 AUTHORS, INCLUDING:

Saadullah G. Aziz
King Abdulaziz University
62 PUBLICATIONS **162** CITATIONS
SEE PROFILE

Elroby Shabaan
King Abdulaziz University
26 PUBLICATIONS **71** CITATIONS
SEE PROFILE

Abdulrahman Al-youbi
King Abdulaziz University
223 PUBLICATIONS **2,621** CITATIONS
SEE PROFILE

Rifaat Hilal
Cairo University
23 PUBLICATIONS **92** CITATIONS
SEE PROFILE

J Mol Model (2014) 20:2078
DOI 10.1007/s00894-014-2078-y

ORIGINAL PAPER

Experimental and theoretical assignment of the vibrational spectra of triazoles and benzotriazoles. Identification of IR marker bands and electric response properties

Saadullah G. Aziz · Shabaan A. Elroby · Abdulrahman Alyoubi · Osman I. Osman · Rifaat Hilal

Received: 22 July 2013 / Accepted: 16 October 2013

Abstract The FTIR spectra of a series of 1H- and 2H-1,2,3- and 1,2,4- triazoles and benzotriazoles were measured in the solid state. Assignments of the observed bands were facilitated by computation of the spectra using the density functional B3LYP method with the 6-311++G** basis set. The theoretical spectra show very good agreement with experiment. Rigorous normal coordinate analyses have been performed, and detailed vibrational assignment has been made on the basis of the calculated potential energy distributions. Several ambiguities and contradictions in the previously reported vibrational assignments have been clarified. "Marker bands" characterize the triazole ring were identified. The effect of substituents, the nature of the characteristic "marker bands" and quenching of intensities of some bands are discussed. Comparison of the topology of the charge density distribution, and the electric response properties of the 1H-, and 2H- isomers of both 1,2,3- and 1,2,4 triazole have been made using the quantum theory of atoms-in-molecules (QTAIM) by calculating the Laplacian of the electron density ($\nabla^2\rho(r)$). Analysis of the contour plots and relief maps of $\nabla^2\rho(r)$ reveals that 1,2,3- and 1,2,4-triazoles show completely different topological features for the distribution of the electron density. Thus, while the 1,2,3-isomer is a very polar molecule, the 1,2,4-isomer is much more polarizable. Bonding characteristics show also different features. This would thus underlie the different features of their vibrational spectra. The reported vibrational assignment can be used for further spectroscopic studies of new drugs and biological compounds containing the triazole ring.

Keywords DFT calculations · IR spectra · Laplacian of the electron density · Polarizibility and hyperpolarizability · Triazoles

Electronic supplementary material The online version of this article (doi:10.1007/s00894-014-2078-y) contains supplementary material, which is available to authorized users.

S. G. Aziz · S. A. Elroby · A. Alyoubi · O. I. Osman · R. Hilal (✉)
Chemistry Department, Faculty of Science, King Abdulaziz University, P.O. Box 80203, Jeddah 21589, Saudi Arabia
e-mail: rhilal@kau.edu.sa

R. Hilal
Chemistry Department, Faculty of Science, Cairo University, Giza, Egypt

S. A. Elroby
Chemistry Department, Faculty of Science, Beni-Suief University, Beni-Suief, Egypt

Introduction

Triazoles and benzotriazoles have been the subject of numerous investigations over the last few decades [1–6]. The interest in this class of compounds continues not only because of the basic chemistry but also because of their biological [7, 8] and industrial [9–15] applications. Triazoles are also particularly interesting molecules from a fundamental point of view since they have been shown to exhibit tautomerism.

Published online: 22 February 2014

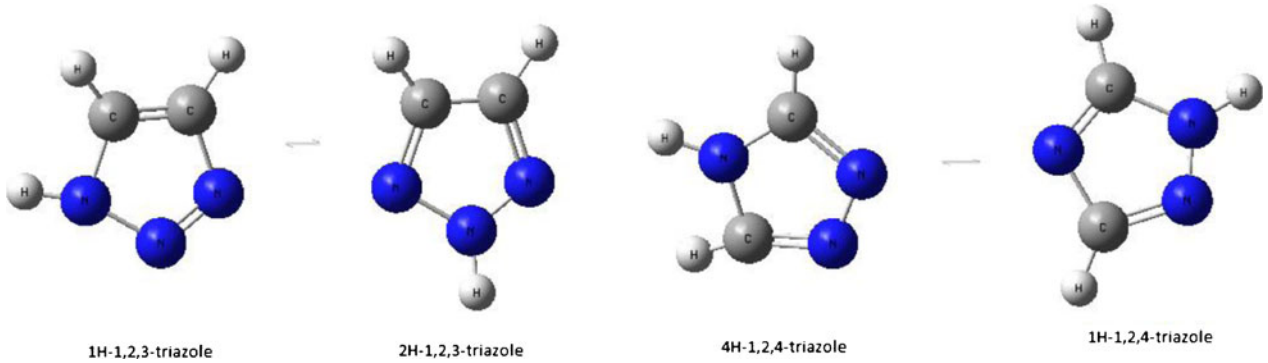

Tautomeric 1,2-proton transfer reaction in triazole, appears to take place on femtosecond to picosecond timescales [16]. In the case of ultrafast condensed-phase chemistry, the dynamics are determined not only by the potential energy surfaces of the reactant-product species, but the surrounding solvent also plays a major role. Attempt to analyze and resolve the 1,2-proton shift in triazoles using x-rays[17], Thermal[18], ^{13}C [19] and ^{15}N[20] NMR spectroscopy failed to arrive at solid conclusions regarding this ultrafast structural dynamics process. An important analysis tool toward the understanding of this ultrafast process of triazoles, is vibrational spectroscopy; in both frequency and time domains. Vibrational transitions can often be correlated to specific vibrational motions by inspection of the transition frequencies. In particular the fingerprint region offers a wealth of structural information. From identification of these fingerprint vibrational modes, conclusions can be drawn on specific structural motifs in the molecules. Vibrational transitions have very small bandwidths (10–20 cm^{-1}), it is thus less probable that different transition bands overlap. Interpretation of such spectra is not straight forward, however. Therefore, quantum mechanical calculations seems necessary in this respect.

In spite of the importance of the subject, quite a few papers that dealt quantitatively with the vibrational spectra of triazoles [21–28]. The one with relevance to the present work is that of Billes et al. [29] who analyzed the vibrational spectra of the parent triazole ring and supported their discussion with DFT calculations. However, no systematic study of substituent effect and consequently no IR markers have been reported so far.

In the present work, the electronic structure and tautomeric equilibria of triazoles will be investigated using FTIR-spectroscopy and DFT quantum mechanical calculations. Effect of substituents on the vibrational spectra will be investigated. Attempt will be made to arrive at IR marker bands for the tautomeric forms of triazoles. In order to quantitatively analyze and discuss the vibrational spectra of triazoles, it is important to investigate the molecular topological features of the electron density. Understanding the charge density distributions and the effect of geometric deformations on the bonding and non-bonding interactions are of prime importance for understanding the origin of the vibrational differences and the substituent effect in the studied triazoles. The quantum theory of atoms-in-molecules (QTAM) [30] in conjunction with high level DFT wave functions are used to compute the electron density $\boldsymbol{\rho(r)}$ and its Laplacian $\boldsymbol{\nabla^2\rho(r)}$ for the ground states of the studied parent triazoles.

Experimental details

Compounds

1H-and 2H isomers of 1,2,3-triazoles and 1,2,4-triazoles and benzotriazoles studied were all of 97 % purity, and all were Aldrich products. The 1H-1,2,3-triazole is liquid, the others are solid. They were used without any further purification.

Measurements

Infrared spectra of the compounds were recorded on a Shimad24 820/PC FT-IR spectrometer within the range 4000–400 cm^{-1}. Samples in the solid state were measured in KBr pellets with 1 cm^{-1} resolution.

Methods of calculation

Ab initio MO calculations were performed using the GAUSSIAN 09 program package [31]. Geometry optimizations were performed using the density functional theory (DFT) method using Becke's three-parameter hybrid functional [32] combined with the Lee-Yang-Parr correlation functional (B3LYP) [33] with the 6-311++G** basis set. The choice of this basis set is due to its flexibility, and the fact that, diffuse p

function on the hydrogen atoms tends to compensate the anharmonic effects of the CH and NH stretches. The force constants were analytically computed at the fully optimized geometries. The wide interest in the vibrational frequencies calculated by DFT method is due to its cost-effectiveness, an RMS accuracy of about 18 cm^{-1} can be attained.

Basis sets that would be used in conjugation with the QTAIM should be of appropriate size and flexibility to be able to give accurate representation of the bonding regions. Therefore, the full study was performed using the 6-311++G** basis set [34–36]. This basis set satisfies the above mentioned conditions. The QTAIM computations have been carried out using the AIMAll software package [37].

Computations of the static dipole polarizabilities and first hyperpolarizibilities were carried out using G09 program.

Results and discussion

Vibrational spectra of 1,2,3- and 1,2,4-triazoles

The experimental spectra of triazoles have been published by Rao [38], while theoretically computed spectra and normal coordinate calculations have been carried out at the HF/MP2/6-31G* level of theory, where no scaling of the force field has been applied [39]. More recently, a theoretical treatment of these spectra have been published using the Becke3P86 functional and the 6-311G(d,p) basis set; no diffuse functions have been used and there was excessive use of scaling factors [29]. Furthermore, their measured spectra is of low resolution specially in the finger print region 1300–600 cm^{-1}. None of these published analyses of the spectra provides complete and comprehensive assignment of the IR spectra of triazoles. Moreover, the literature does not seem to reach a conclusion to identify "marker bands" for this biologically important class of compounds. Figure 1A, 1B, and 1C present the IR spectra measured as KBr pellets, for 1H-1,2,3-triazole, 1H-1,2,4-triazole and 2H-1,2,4-triazoles, respectively.It is striking to notice how different are the general features of these three spectra are. The 1H- and 2H-1,2,4-triazoles show quite different spectra specially in the high frequency region, 1H-1,2,3-triazole shows a very broad band system in 3500–2500 cm^{-1} region. The band envelop encloses the N-H stretching, the C-H symmetric and asymmetric stretching bands. Table 1 presents a comparison between the experimentally measured and the theoretically computed spectra of the studied parent triazoles. Data in this table focus on some key vibrations only. Careful inspection of these data reveals the following:

1- There is a general tendency for the theoretical model to overestimate the vibrational frequencies, this is specially apparent in the case of the N-H stretching mode. However, using a scaling factor of 0.965, improves the overall correspondence considerably.
2- The B3LYP/6-311++G** calculation predicted a marked separation between the NH and CH stretching modes of 635, 464, 450, and 408 cm^{-1} respectively for the 1H and 2H isomers of 1,2,3- and 1,2,4-triazoles respectively. Let us investigate these vibrational modes a little bit further. In all four forms the NH stretching mode is almost pure and does not couple with any other mode and is observed at ~3200 cm^{-1} (theoretical value 3500±5 cm^{-1}). The very narrow range indicates and reflects the almost constant environment of the NH group. On the other hand, the CH stretching mode shows marked variations. Thus, for 2H-1,2,3-triazole, both the symmetric stretch and the asymmetric stretching modes are very much overlapping ($\Delta\nu$ = 20 cm^{-1}) both are pure and no coupling is observed. On the other hand, in the case of the 1H-form the symmetric and asymmetric CH stretch are more resolved and show a slight shift to higher frequency regions ($\Delta\nu$ = ~50 cm^{-1}). This shift is probably due to the accumulation of electron density in the N=N bond region. This, also causes coupling of the CH symmetric stretching mode with the C-N and C = C and some other ring breathing modes. For all four forms of triazole, the CH vibrational modes are much less populated than the NH mode. This is reflected in the extreme low relative intensities of the CH modes.
3- A strong combination band is observed experimentally at 1208 cm^{-1} and predicted theoretically as a doublet at 1283 and 1175 cm^{-1}. This band may be assigned to a combination of the N=N, C-N stretching modes in combination with some ring breathing vibration. For 2H-1,2,3-triazole, on the other hand, a complex band structure spans the 1262–1180 cm^{-1} range, is predicted. This band structure may be assigned to the same combination, yet with reduced intensity.
4- 1H-1,2,4-triazole is predicted theoretically to have a manifold with two main strong peaks at 1461 and 1386 cm^{-1}. This manifold is due to the N = N and C-N stretching and combination of CH and NH angle bending. This manifold suffers intensification and shift to higher frequencies in the 2H isomer. The correspondence between the theoretically calculated and experimentally observed frequencies for this mode is less satisfactory.
5- It is interesting to notice that the ring disruption (deformation) modes for the four forms are predicted almost in the same frequency range (995–955 cm^{-1}) and as a pure non interacting mode. This ring mode, is not affected by the 1H and 2H tautomerization and also independent of the arrangement of the nitrogen atoms.
6- The interpretation of the vibrational spectra of triazoles, in the low frequency region, is difficult since the spectra

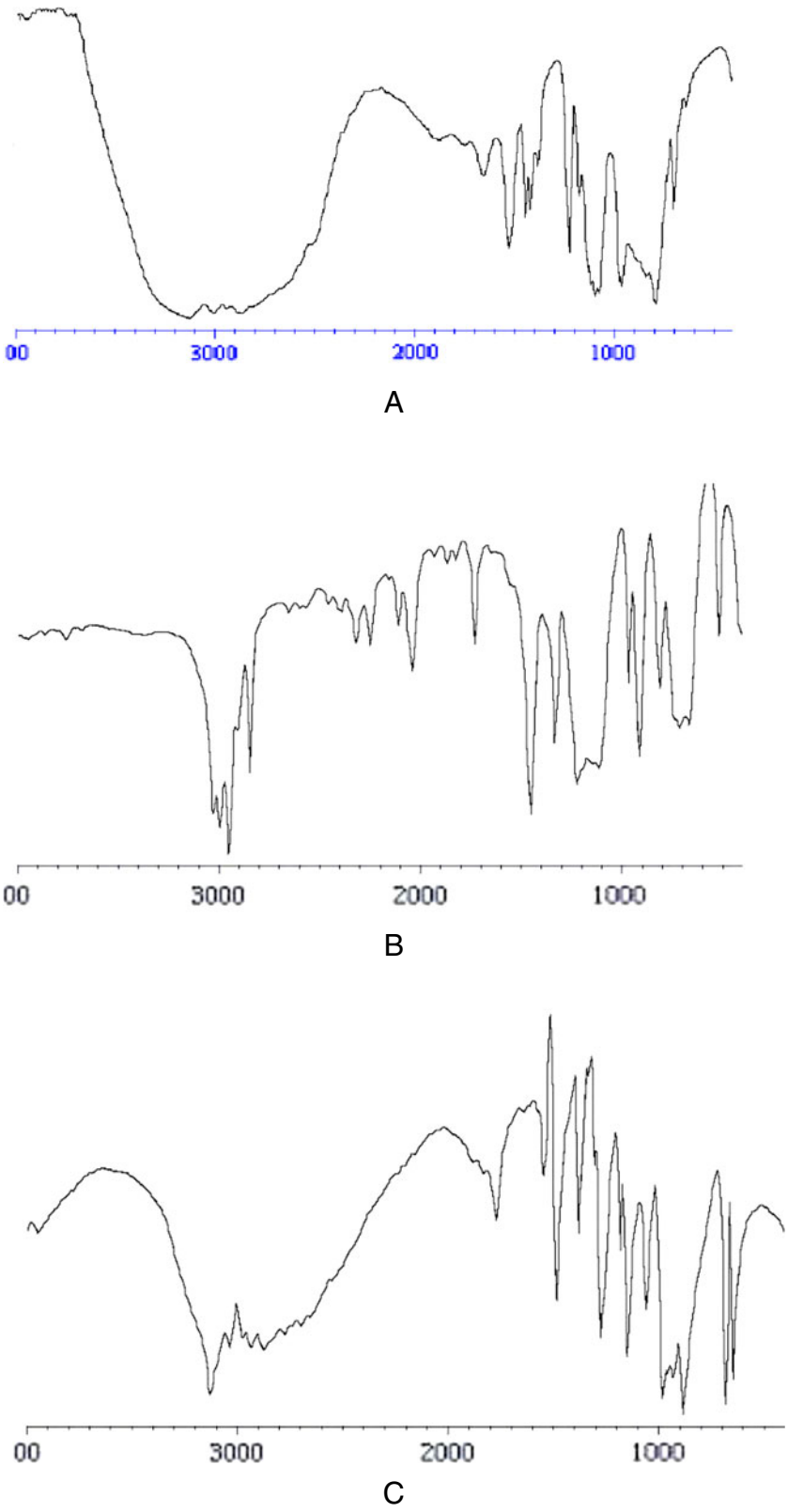

Fig. 1 FTIR spectrum of **A** 1H-1,2,3-triazole **B** 1H-1,2,4 triazole and **C** 2H-1,2,4-triazole measured in KBr palette

reflect the very strong associations in condensed state and is full of overlapping broad bands which makes the assignment of the observed bands not straightforward. Theoretically, however, one can identify a manifold of

Table 1 Comparison between theoretically computed and experimental IR spectrum of the studied parent triazoles

Assignement	1H1,2,3-triazole			2H1,2,4-triazole		1H1,2,4-triazole		2H1,2,3-triazole[a]			4H1,2,4-triazole		
	ν,cm^{-1}	%	Exp.	ν, cm^{-1}	%	ν, cm^{-1}	%	ν, cm^{-1}	%	Exp.	ν, cm^{-1}	%	Exp.
N-H Str.	3500	100	3160	3740	100	2820	99	373	93	3040	3676	96	3130
CH sym. stretch	3150	60	3000–2760	3396	99.0	3374	99	3406–3393	89–92	3000–2840	3402	87–85	3040–2700
CH asym. stretch	3130	99.25		3381	99.0	3345	99				3386		
C = N,C = C str, N = N tr.	1529	6.5, 13, 33, 41		1490	35	1446	19	1662	33, 43, 16		1655	39, 0, 45, 17	
NH,CH in p. bend					61, 0		6, 74						
CH in-plane bending	1324	74	1208	1321–1176	26–64	1251	98–0.5	1295	79–25	1208	1234	80	1265
NH bending N = N st.		18			70–14							13	
Ring disruption	1005–966	99.2–92.3	975	1006–979	98–99	997–934	94–96	1005–970	39–35	795–730	1008–973	79–43	790–650
			955							710–665			
Out-of-plane torsion	724	99–98		851–798	99–99	807–773	93–98	855–798	90–92		856–798	70–90	
	652	96–94		692–665	87–97	666–634	54–89		84–79		677–652	92–89	
	569												

[a] Reference [27]

three strong bands of intensities varying between strong and medium, in the region 750-550 cm^{-1}. This manifold can be safely assigned to the out-of-plane ring deformation coupled with the N-H out-of-plane bending modes.

In conclusion, the predicted vibrational spectra of 1H-, 2H-1,2,3- and 1,2,4 –triazoles correspond satisfactorily to the experimentally observed IR spectra of these compounds. Using a scaling factor of 0.965 seems to improve the correspondence with the experimentally determined spectra. Figures 2 and 3 present some selected vibrational modes for 1H-,and 2H-1,2,3-triazole and 1H- and 2H-1,2,4-triazole. The spatial presentation of these modes is very illustrative. Thus, in all three compounds the pure nature of the NH- stretching mode is very illustrative. The coupling between the NH- and CH- bending modes is very well illustrated in figure 1(c). However, this bending mode is coupled with ring vibrations which are most probably responsible for the observed shift to lower frequencies. The ring disruption mode figure 2(d) is strongly coupled with CH- and NH- bending modes. It is interesting to pinpoint the difference between the general features of the ring disruption mode of 1H- and 2H-1,2,4-triazole. 1H-1,2,4-triazole shows a highly asymmetric vibration which is markedly different from that of the 2H-form.

Electric response properties and the topology of the electron density

In spite of the importance of triazoles in biology and in industry, yet very little is known about their electric response properties [40] and nothing is known about the underlying topology of their charge density distribution. The development of the theory of electric multipole moments and polarizibility [41, 42] has made a decisive contribution to our understanding of fundamental phenomena in many areas of importance to molecular science [43]. Of special interest is the systematic use of electric polarizibility in modeling the pharmacological activity of molecular substances [28] and in quantitative structure-activity relationship (QSAR) studies [44]. In this section we report and discuss some electric response properties, namely dipole and higher multipole moments, polarizibility and first hyperpolarizibility for the studied triazoles in conjugation with analysis of the electron density based on the quantum theory of atoms-in-molecule (QTAIM).

Table 2 presents the electric response properties computed in the present work for the 1H- and 2H- 1,2,3- and 1,2,4-triazoles studied in the present work. 2H-1,2,4-triazole has its dipole moment vector coinciding with the N-H bond vector and thus has the largest dipole moment of all forms studied. 2H-1,2,3-triazole, on the other hand, has the smallest dipole moment. This can be further analyzed by inspection of figure 4 which displays the molecular graphs of 1H-1,2,3- and 1H-

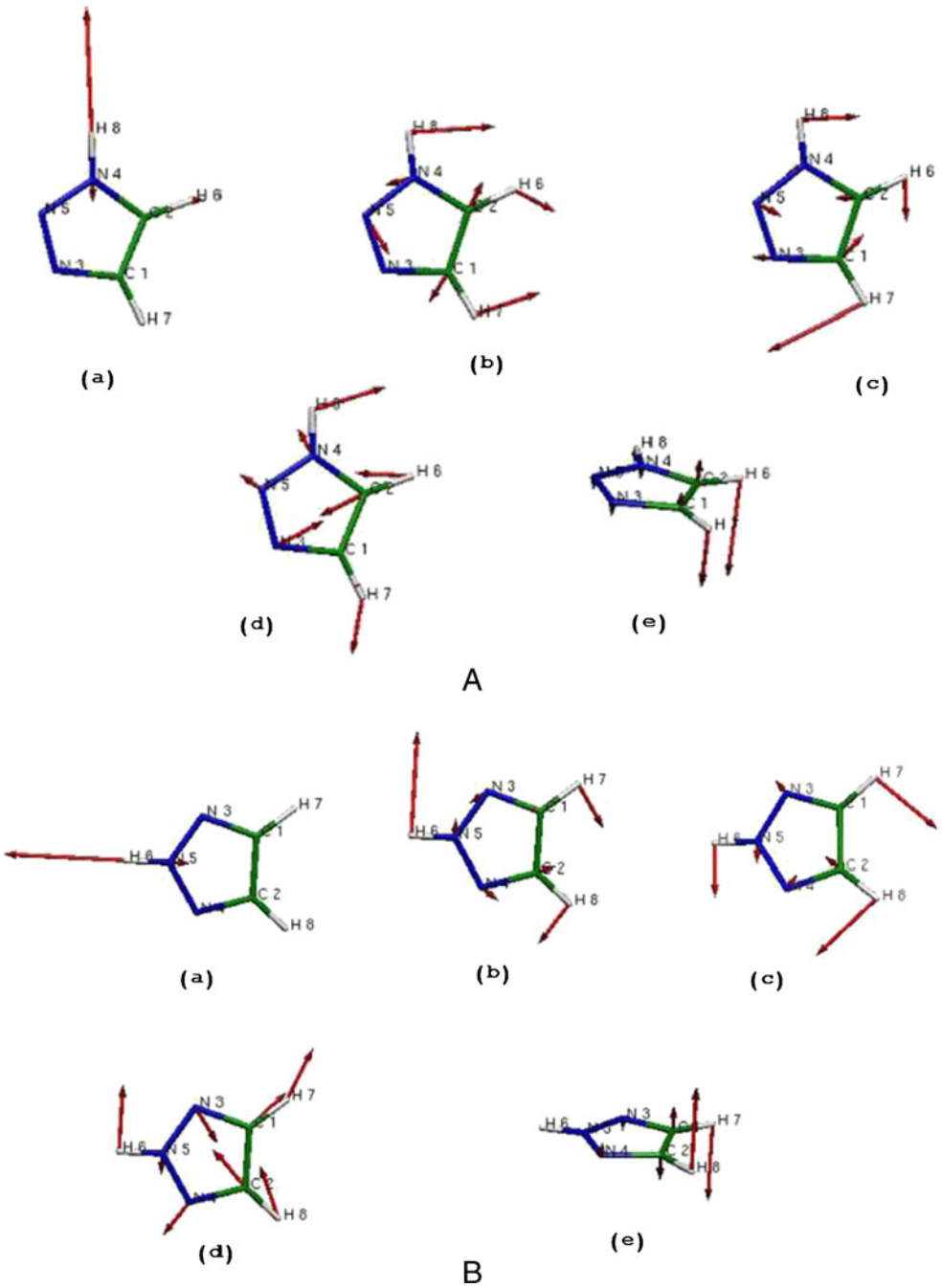

Fig. 2 Comparison of the calculated atom displacements associated with normal modes **A** 1H-1,2,3- triazole and **B** 2H-1,2,3-triazole

1,2,4-triazoles as computed at the QTAIM/6-311++G** level of theory. These molecular graphs display a comparison between the AB components of the dipole moments in 1H-1,2,3- and 1H-1,2,4-triazoles. The dipole moment is not only reduced by a factor of 2 on going from the 1H-1,2,3- to the 1H-1,2,4- isomer, but its components show also different trends. It seems that in 1H-1,2,3- triazole all N atom dipole components add into a resultant in one direction whereas in the case of the 1,2,4- isomer there is scattering of these components. The quadrupole moment tensors elaborates on this trend. The 1H-1,2,4- triazole ring seems highly polarizable with appreciable components in the three directions. At this point it seems interesting to note the trends in the values of the theoretically computed polarizabilities. The position of the H- atom has a marked effect on the magnitude of the polarizibility. Thus, 1H-1,2,3-triazole has a static dipole polarizibility, α, greater than that of the 2H-isomer. The same trend is also observed for 1H- and 4H-1,2,4-triazoles. Furthermore, the value of α computed for 1,2,3-triazole is greater than that computed for the 1,2,4-isomer. This same trend holds on a magnified scale for the first hyperpolarizability, B_{total}, values computed for the studied triazoles. The longitudinal

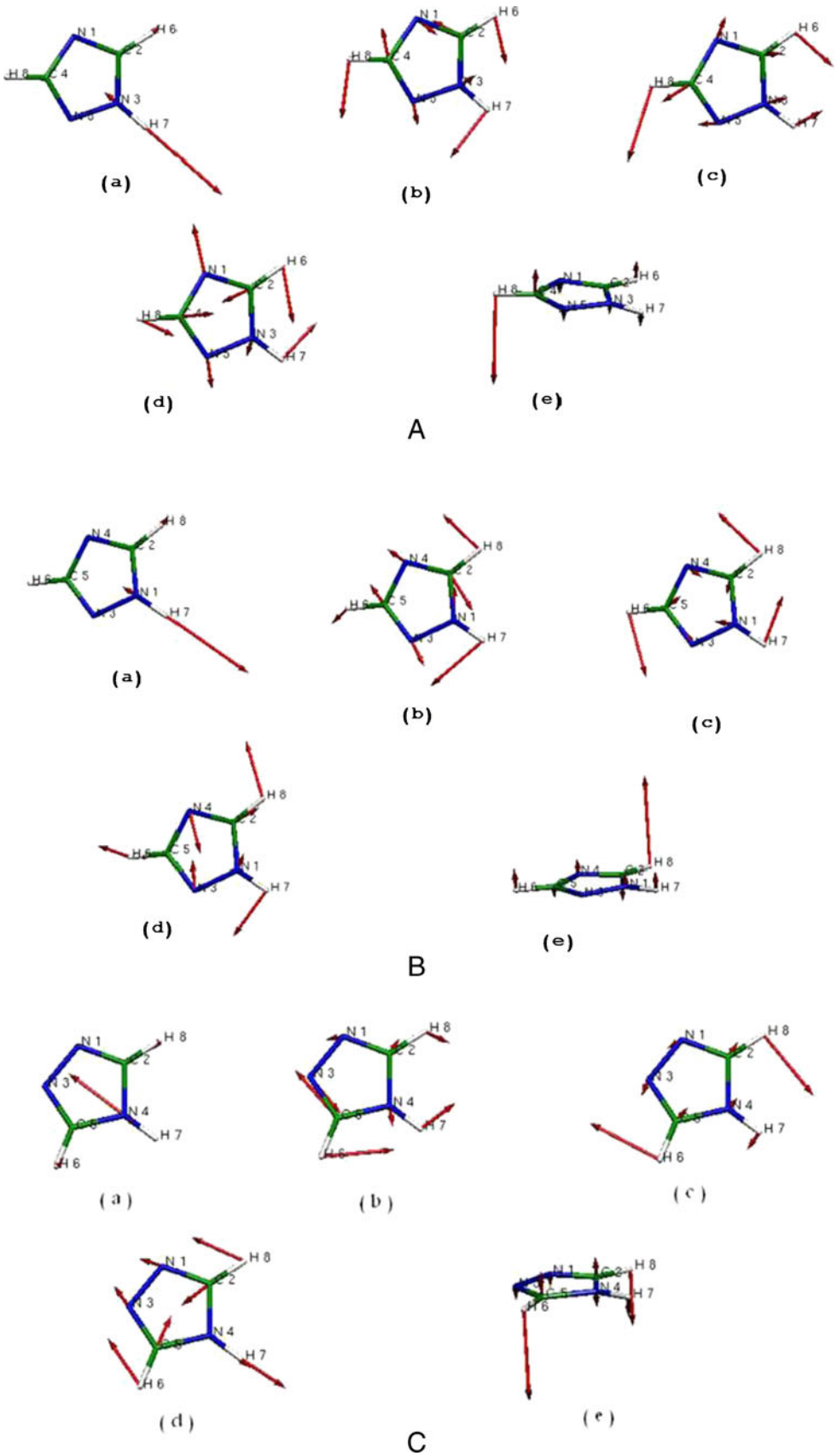

Fig. 3 Comparison of the calculated atom displacements associated with normal modes **A** 1H-1,2,4-triazole **B** 2H-1,2,4-triazole and **C** 4H-1,2,4-triazole

Table 2 Electric response properties computed at the DFT/B3LYB/6-311++G** level for the studied 1H- and 2H- 1,2,3- and 1,2,4-triazoles

Property	Tensors	1H-1,2,3-	1H-1,2,4-	2H-1,2,3-	4H-1,2,4-	1Hbenzo 1,2,3	2H-benzo 1,2,3
μ, D		4.6062	2.5434	0.2105	5.8522	0.2637	3.9923
Spatial extent R^2		269.59	295.32	268.25	269.39	959.2012	964.1418
Quadruple moment (Debye-Ang)	xx	−23.5505	−20.7282	−33.9211	−25.7815	−39.2570	−52.0394
	yy	−31.1440	−35.3357	−20.8301	−29.3324	−51.7628	−44.0640
	zz	−30.6929	−30.8087	−30.5938	−30.4420	−52.9374	−53.3083
Polarizability α	xx	49.4480	49.152	47.590	49.800	119.220	126.481
	yy	49.2580	47.2170	49.559	47.495	94.991	97.538
	zz	27.9317	27.250	27.6404	27.3896	48.926	51.187
Average <α>		42.2126	41.2130	41.60	41.56	87.71	91.74
Δα		21.5163	21.902	19.949	22.401	70.294	75.294
B_{total}		54.436	26.606	34.593	8.139	73.091	89.419

Polarizability α in $Bohr^3$, hyperpolarizability B_{total} in **au**

component tensor, αxx, is prevailing in all triazoles studied. Notice that the symmetry of 1,2,3-triazole is reflected in an equal in-plane components α_{xx} and α_{yy}. The out-of-plane tensor α_{zz} although smaller in magnitude is still of appreciable value and reflect the polarizibility of the π system. The dipole hyperpolarizability, β, on the other hand, is much more

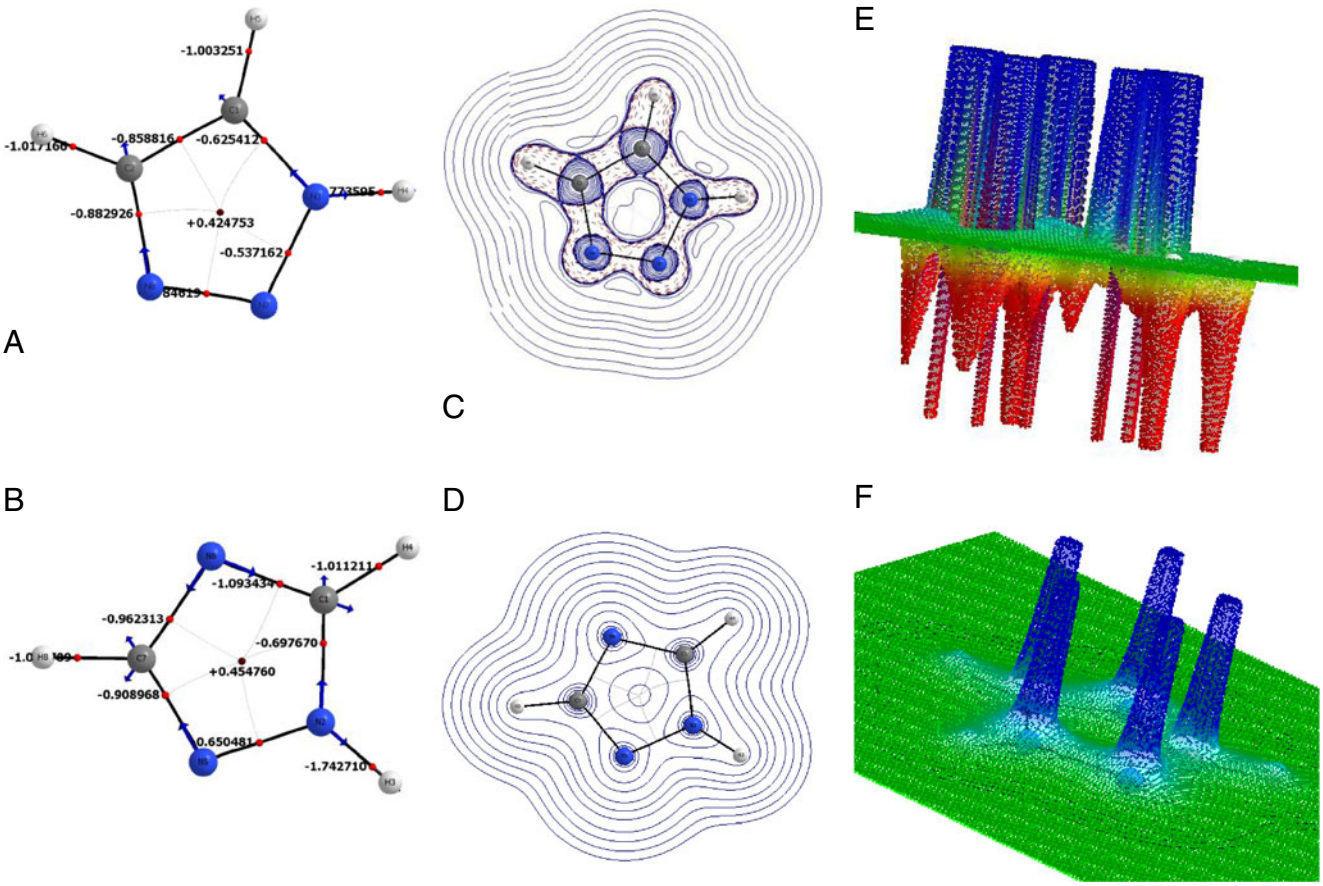

Fig. 4 Molecular graph of **a** 1H-1,2,3 triazole and **b** 1H-1,2,4-triazole. The color scheme in this and all following graphs is as follows: nitrogen atoms are in blue, carbons in dark gray, and hydrogen in light gray color. Bond critical points (BCP) in small red spheres, ring critical point (RCP0 in brown. Values of $\nabla^2\rho(r)$ are given at each CP. Blue arrows indicate contribution of atom (A) dipole moment to the A-B bond moment. **c** and **d** contour plots of $\nabla^2\rho(r)$ and **e** and **f** are relief maps of $\nabla^2\rho(r)$ plotted in the molecular plan for, 1H-1,2,3-triazole and 1H-1,2,4-triazole, respectively. All computed at the QTAIM level using the 6-311++G** wave function

sensitive to the structure and molecular volume. It seems important to examine the frequency dependence of the polarizibility. When a charge-distribution is hit by a monochromatic electromagnetic wave with electric component $\mathbf{E}_{\cos\omega t}$ **the polarizibility becomes a function of the angular frequency.**

$$\alpha(\omega) \text{ with } \omega = 2\pi\nu = kc,$$

where ν the frequency, *k* the modulus of the wave vector and *c* the speed of light. We have compute α, for 1H-1,2,3-triazole, at frequency ω=0.1 au. The computed value is 44.66 $Bohr^3$ with an increase of about 2.5 $Bohr^3$ from its static value; all three tensor components are effect. At a frequency ω=0.016 au (corresponds to the frequency of the N-H stretch in triazoles) the computed value is 42.27 $Bohr^3$ with a slight increase of only 0.07 au from its static value.

The contour plots and the relief maps, of the Laplacian of the electron density in the plane of the triazole ring, in figure 4 are also very illustrative in this respect. The topology of the charge density in 1,2,3 and 1,2,4-triazoles are completely different. The dotted contour lines in figure 4a correspond to regions of local charge concentration; such lines are markedly dimensioned in figure 4b. Note, in figure 4a the concentration of charge on and around the heteroatoms and specially in the middle of the ring. This is probably more evident in the relief map displayed in figure 5e. The nuclear maxima in the density have been terminated at 4 au and the map boundary at 0.001 au. Note the presence of "saddles" in the density between bonded atoms. The presence of maxima in the density at the positions of the nuclei is the dominant topological feature of the electron density. The maxima pointing downward are those due to accumulation of charge in the bonding regions which seem absent to a large extent in figure 4f. In figure. 4e the nitrogen atoms show the widest accumulation of charge and there is in addition to the maxima at the nuclear positions, accumulation of charge in the bonding regions. The distribution of these maxima in the valence shell charge concentration (VSCC) reveals tight binding and polarization of the charge density. While the charge accumulated in N-N-N bond region exceeds that in any other region in the molecule, all nitrogen atoms have significant residual valence density; that is particularly evident in the large non-bonded charge distribution on C. It imparts to C a large 'back polarized' atomic dipole that results in a near vanishing molecular dipole moment. Thus, the charge distributions of the nitrogen atoms approach their 'ionic' limit. Some selected bonding parameters are displayed in Table (1S) and (2S) of the supplementary material.

In conclusion, inspection and analysis of the $\nabla^2\rho(r)$ reveals that 1,2,3- and 1,2,4-triazoles show completely different topological features for the distribution of the electron density. Thus, while the 1,2,3- isomer is a much more polar molecule the 1,2,4-isomer is much more polarizable. Bonding characteristics show also different features. This would thus underlie the different features of their vibrational spectra.

Effect of substituent on the vibrational spectra of 1,2,3-triazole

Table 3 presents the vibrational spectral characteristics of 5-ethyltriazole calculated theoretically at the DFT/B3LYP level of theory. This spectrum dose not resemble that of the parent molecule 2H- 1,2,3triazole. The effect of the ethyl substituent can be traced in causing a general shift to lower frequencies. In the case of CH stretch, the electron donating effect, by induction, of the ethyl group causes an increase in the electronic density and hence the frequencies shift to lower values. Furthermore, due to the steric effect of the ethyl group, the CH in-plane bending and out-of-plane bending bands show further shift which has also been predicted theoretically.

Two electron-donating substituents have been investigated, namely, the diamino- and the tolyl groups (Table 3). Substitution by any of these groups into position 4 and/or 5 of the triazole ring causes polarization of both the σ - and the π - frame works. These polarizations are opposite in direction. The donating tendency of these groups causes extended delocalization of the π- framework and hence increase of the π - bond order in the X-triazole bond region. This will consequently cause an increase in the N-H force constant. This increase in k accounts for the observed shift of CH to higher values. The two amino groups, in case of diamino triazole, act as electron donating groups, so the NH and CH stretching modes suffer a marked shift to higher frequencies as compared to the corresponding mode in 2H −1,2,3triazole.

The tolyl moiety, in the case of tolyl triazole, follows the same trend and shifts the frequency of CH and the NH stretching modes of the five membered ring to higher values. The CH in-plane bending, is predicted theoretically as a pure vibration mode at 1209 $cm^{-1,}$ in close agreement with the experimental value. The frequency of the CH out-of-plane bending frequency, seems much more sensitive to steric effect of the substituent.

Chlorine substitution in tolyltriazole (Table 3) shifts the NH stretching frequency to lower frequency by 12 cm^{-1} due to electron withdrawal effect. Chlorine substituent also causes increase of electronic density near the triazole ring with the consequent increase in the frequency value of the triazole ring. Introduction of hydroxyaminomethyl group into tolyltriazole shifts the CH stretch frequency to lower values due to steric effect.

In conclusion, we have examined our theoretical model against the experimental spectra of some simple substituted triazoles. The aim is to focus on the capability of the model to

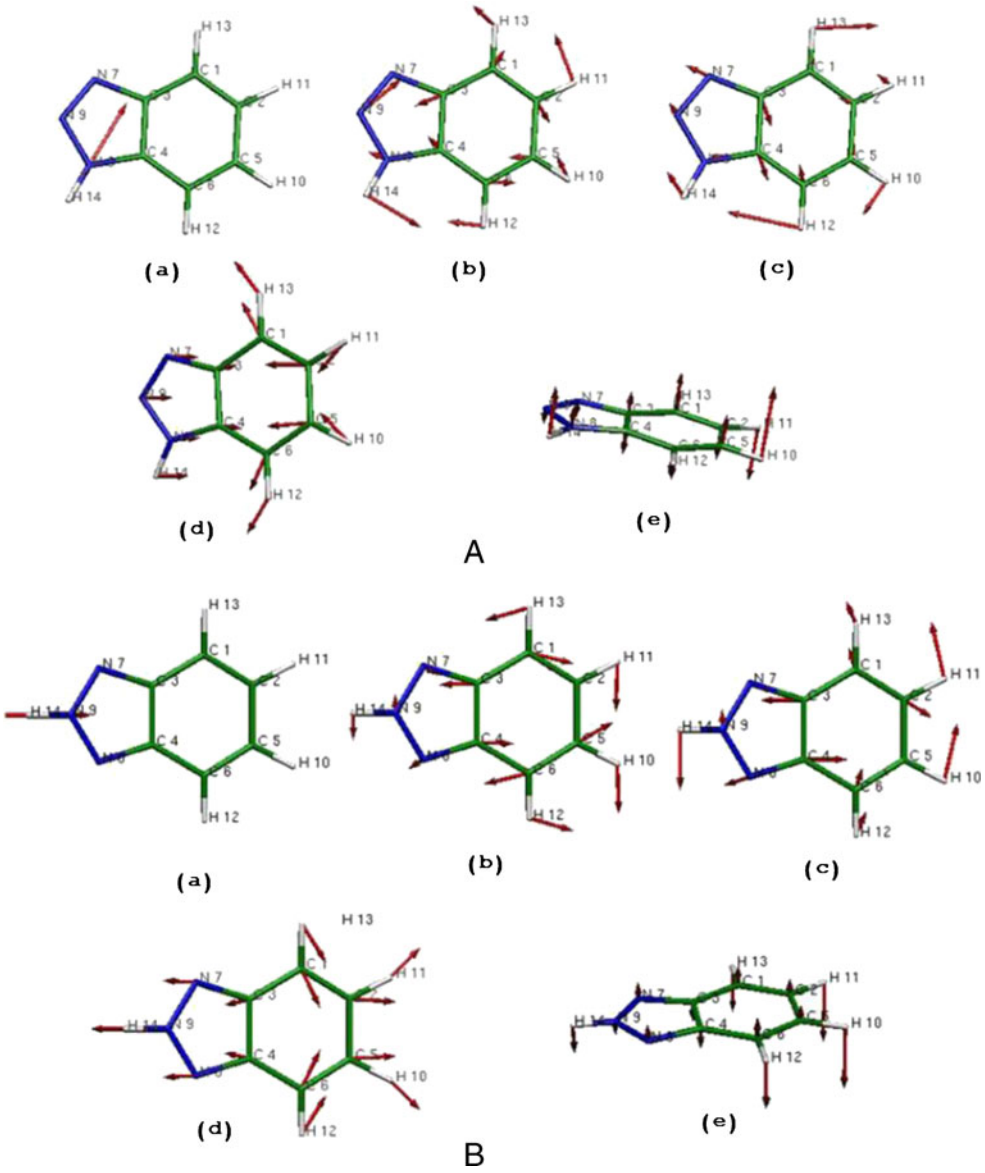

Fig. 5 Comparison of the calculated atom displacements associated with normal modes **A** 1H benzotriazole and **B** 2H-benzotriazole

predict changes in the spectra due to electron withdrawing/donating effect of the substituents studied. The present theoretical model proved its capability to capture these effects and the overall correspondence with the experimental spectra is satisfactory.

Vibrational spectrum of benzotriazole

The literature contains several ambiguities and contradictions concerning the benzotriazole tautomer prevailing in condensed phase or in the gas phase. In addition, there are also ungrounded assumptions as to the existence of appreciable percentage of a quinonoide form of 2-H benzotrazole [45, 46]. In the following we will attempt to analyze and discuss the vibration spectra of benzotriazoles and address these points. The experimentally measured spectra of benzotriazoles are displayed in figure (2S) of the supplementary materials. Table 4 presents the theoretically calculated IR spectra of benzotriazoles at the DFT/6-311++G** level of theory. Careful examination of the data presented in Table 4 reveals that the presence of the fused benzene ring causes a marked shift toward higher frequencies for the NH- stretching mode. Thus, in the case of 1,2,3-triazole, the NH- absorption is predicted at 35,000 cm^{-1}, some 130 cm^{-1} lower than that predicted in the case of 1H-benzotriazole and ~150 cm^{-1} lower than that predicted for the 2H-benzotriazole. The CH- stretching mode shows almost the same trend, however. Thus, while, 1,2,3-triazole shows both the symmetric and asymmetric CH- stretching modes at 3245 and 3229 cm^{-1}, respectively, benzotriazoles show their CH stretching mode at 3320 cm^{-1}, shifted some 100 cm^{-1} to higher frequencies. It is interesting, however,

Table 3 Comparison between theoretically computed and experimental IR spectral characteristics of the studied 1,2,3-triazole derivatives

Assignement	Ethyl triazole		diaminotriazole		p-Tolyltriazole		5-Chloro p-tolyltriazole		5-hydroxaminotolyltriazole	
	ν,cm^{-1}	%	ν, cm^{-1}	%	ν, cm^{-1}	%	ν, cm^{-1}	%	ν, cm^{-1}	%
O-H str.									4086	99
N-H Str.	3709	99	3712	99.8	3706	100	3695	99.7		
CH sym. stretch ring	3387	99.5			3422	99.8	3430	96.5	3375	98.8
CH3 sym. stretch	3248–3232	96–97			3344–3326	98–97	3367–3342	96–98	3348	98
Asym CH2 str	3163	97.5			3304–3302	99–98	3324–3293	99–97	3310–3293	98–95
Sym CH2,CH3 str	3158	47–52			–	–	3259	98	–	–
Sym CH2 str	3132	54			–	–			3311	99
CH(3) asy Str.					3256–3237	98–99			3253–3235	96–95
CH(3)sym Str.					3166	97				
C = N str, N = N str.	1524	7	1678	17	1495	11–10	1489	8,3,4 1,66	1477	25,40 30,0,0
NH,CH in p. bend		5–54		0		62–17		–		
NH2 in-plane bending				80						
CH in-plane bending	1276	45	1273		1209	81	1207	92	1210	98
NH bending		20		62.5		–				
N = N st.		21				–				
Ring disruption	1071–1020	78–62	1099–995	94–91	1034–903	48–45	1044–1033	69–75	1081–1051	43–50
	983–661	56–42	804–690	97–95	823–792	32–51	995–843	66–66	1049–1013	58–50
					618	55	775–655	43–54	1009–821	39–55
								49	658-637	73-90
CH out-of-plane bending	323–758	91–85			1046–903	92–95	941–922	94–96	1046–929	96–98
	689–657	62–64			823–792	89–95	821–791	95–96	914–827	91–96
									798–715	95–91.5

to notice that the main combination band appears in the spectrum of triazole at 1529 cm^{-1}, is predicted to be present at the same frequency (1599 cm^{-1}) in the case of 1H-benzotriazole and is a combination of the C = C, C = N stretching and CH and NH in-plane bending modes. This combination band is predicted to appear at 1400 cm^{-1} in the case of 2H-benzotriazole. Figure 5 displays a comparison of the calculated atom displacements associated with normal modes of "marker bands" characterizing the IR spectra of 1H-benzotriazole and 2H-benzotriazole. Note also, in

Table 4 Comparison between theoretically computed and experimental IR spectral characteristics of the 1H and 2H-benzotriazoles

Assignement	1H-benzotriazole					2H-benzotriazole				
	ν, DFT	%	ν, HF	%	ν, Exp.	ν,DFT	%	ν,HF	%	ν,Exp.
NH stretch	3624	100	3885	98	3210	3658	99.5	3882	90.7	3280
CH Strech									4.5	
CH symm Str.	3323	97	3395	89	3150	3323	97.8	3394	97	3100-2700
CH asymm. Str.	3322–3240	97–98	3394–3307	85–80	2930					
N = N,C = C,C = N str.	1414	1:5:6	1492	48	1260	1599	8.5	1440	0-0-8	
NH,CH, in-plane bending		13-79		41, 0			3`1.3		25–13	
CH in-plane bending	1247	52	1255	48	1260	1274	48.5	1251	79	1208
NH bending		43.6		41			6.8			
N = N Str.		1.7					5.4			
Ring disrubtion	1044–998	97–96	1061–988	54–48	860–675	1046–643	96–98	90–844	90–93	860–750
CH out-of-plane bending	974–936	99–78	877–723	78–43		960–914	80.2–92	860–850	84–73	
	852–737	96–95	639	57		832–765	94–96	638	90	
	681	90.5								

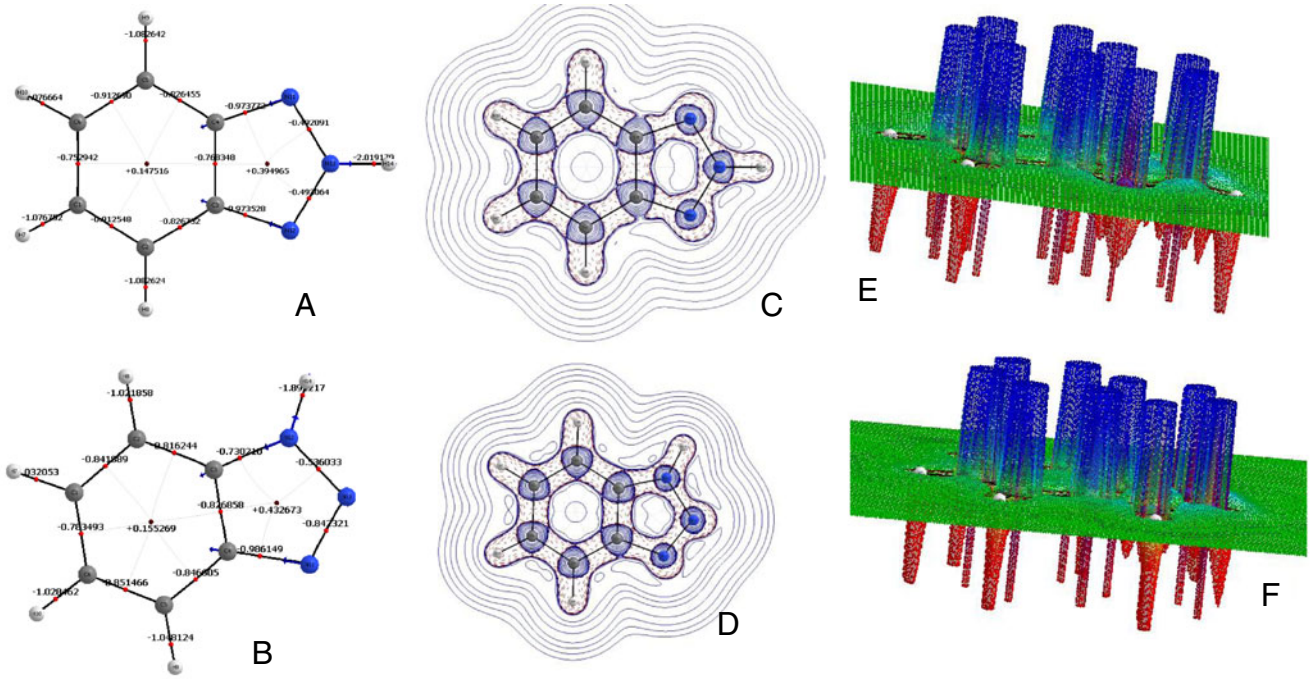

Fig. 6 Comparison of the topological features of $\nabla^2\rho(r)$ for 1H and 2H-benzotriazoles. **a** and **b** are the corresponding molecular graphs **c** and **d** are contour plots of the Laplacian of the electron density and **e** and **f** are the corresponding relief maps

addition to the ring combination band mentioned above, the triangular ring breathing mode that appears in the 1000–850 cm^{-1} range with almost the same medium intensity of 33 KM/mol. In all triazoles studied so far, the N-H stretching mode is pure uncoupled, its position and intensity is but little affected by substitution.

The electric response properties computed for 1H- and 2-H benzotriazoles are compiled in Table 2. The trends observed for the polarizibility and hyperpolarizability are the same as that discussed in the case of the parent triazoles. The characteristic bonding properties computed from analysis of the wave function and the Laplacian of the electron density are summarized in Tables (3S) and (4S) of the supplementary data. Figure 6 presents a comparison of the topological properties, contour and relief maps of 1H- and 2H-benzotriazoles. It is clear that the two molecules exhibit the same topological features of their electron density distributions. Furthermore, the accumulation of the valence charge density seems

Table 5 Comparison between the theoretical and experimental vibration modes computed at the DFT/B3LYB/6-311++G** level for the studied benzotriazoles substituted by electron donating substituent

vibration mode	5-methyl		1-hyroxy		4-hyroxy		5-hyroxy-	5-amino-	
	Calc.	Exp.	Calc.	Exp.	Calc.	Exp.	Calc.	Calc.	Exp.
ν_1 N-H str.	3732	3100			3733	3280	3733	3733	3400
ν_2 C-N str.	1362	1380	1398	1420	1452	1385	1370	1364	1340
			1322		1311	1360		1288	
ν_3 N = N + N-H bending + ring breathing	1331	1310	1349	1380	1296	1300 1285	1319	1322	1300
ν_4 ring breathing	1294	1290	1276	1310 1180	1260	1210	1277	1255	1250
ν_5 N-N str.	1026	1020	1070	1030	1032	1060	1024	1033	140
		985	979	1010	1000	1010	993	993	1020
ν_6 Ring disruption	897	940	910	840	893	910	896	897	885
		860		685					
ν_7 ring out-of-plane torsion	791	760	781	780	797	785	773	775	760
	695	670	636	750	689	760	693	695	680
		600		740		740			600

Table 6 Comparison between the theoretical and experimental vibration modes computed at the DFT/B3LYB/6-311++G** level for the studied benzotriazoles substituted by electron withdrawing substituent

Vibration mode	BTA	5-chloro-		1-chloro		5-Nitro	5-carboxyl
	Calc.	Calc.	Exp.	Calc.	Exp.	Calc.	Calc.
ν_1 N-H str.	3708	3732	3550			3732	3733
ν_2 C-N str.	1405	1460	1470	1623	1450	1458	1462
		1318		1506		1264	1372
ν_3 N = N + N-H bending + ring breathing	1304	1318 1275	1300	1380	1380	1240	1334
	1278			1272			
ν_4 ring breathing	1243	1252	1240	1118	1150	1278	1243
ν_5 N-N str.	1199	1020	1005	992	1020	1048	1025–992
	883	992	980		1005		
ν_6 Ring disruption	984	895	910	899	880	873	895
ν_7 ring out-of-plane torsion	781	786	740	644	740	668	780
	699	696	690	569	610	617	692

independent of the position of the hydrogen atom. One thus would expect the same features for their vibrational spectra and the same substituent effects.

Effect of substituent on the vibrational spectra of benzotriazole (BTA)

In the following we will attempt to investigate the effect of substituents of varying electron donating/withdrawing tendency on the vibration spectra of benzotriazoles. Special emphasis will be given to the behavior of the selected "marker bands" of the triazole ring. Three electron donating groups, namely $-CH_3$, OH and NH_2, and three electron withdrawing groups, namely -Cl, $-NO_2$ and -COOH,will be considered. Comparisons between the theoretically computed and experimentally observed vibrational frequencies are given in Tables 5 and 6. The corresponding FTIR spectra are displayed in figure (2S) of the supplementary material. In all benzotriazole derivatives studied, the N-H stretching mode appears pure, and uncoupled at almost constant frequency which is some 80 cm^{-1} higher than that of triazole itself and less than 30 cm^{-1} higher than that in the case of benzotriazole. Furthermore, it is interesting to notice that the ring disruption mode ν_6 appears as a medium intensity band at almost the same frequency for all benzotriazole derivatives studied. This mode is slightly shifted to lower frequencies as compared to its frequency in case of the parent benzotriazole. The same trend may also be noted for the strong N-N stretching mode ν_5 which spans a very narrow range from 990–1070 cm^{-1} for all studied derivatives. These two bands are highly characteristic and identify the triazole ring in addition to ν_1, the N-H stretching mode.

The behavior of the combination band ν_3 needs, however, careful analysis. Subsituents in position 1, whether electron withdrawing such as the –Cl or electron donating such as –OH, cause a marked shift, in the position of this vibration

Table 7 Electric response properties computed at the DFT/B3LYB/6-311++G** level for the studied substituted benzotriazoles

Property	Tensors	5-methyl-	1-hyroxy	4-hyroxy	5-hyroxy-	5-amino-	5-chloro-	1-chloro	5- nitro	5- carboxyl
μ,D		4.59	2.85	3.47	5.67	4.60	4.40	5.15	6.89	5.14
Q,, (D-degree)	XX	−58.09	−43.77	−63.11	−55.17	−58.70	−67.39	−71.9	−56.82	−71.98
	YY	−55.94	−61.03	−47.91	−53.14	−53.25	−59.76	−57.1	−68.36	−57.13
	ZZ	−62.22	−60.42	−60.42	−60.43	−61.11	−66.54	−66.4	−70.29	−66.40
α	XX	160.2	138.1	138.4	137.9	143.6	154.8	175.2	292.3	175.2
	YY	112.8	106.9	102.5	102.4	104.6	105.9	112.9	129.6	112.9
	ZZ	72.7	54.1	53.2	53.2	56.3	57.6	61.4	75.4	61.40
$\alpha_{average}$		114.89	99.70	98.03	97.83	101.50	106.10	116.5	165.77	116.5
< α >		87.5	84.0	85.2	84.7	87.3	97.2	113.8	216.9	113.8
β_{TOTAL}		554.64	53.80	445.84	279.08	80.73	192.22	233.14	5902.47	592.80

Polarizability are in $Bohr^3$, hyperpolarizability are in**. au**

mode, to higher frequencies. This shift seems to be independent of the type of the substituent but rather on its molecular (atomic) mass. In both cases studied, the substituent has a reduced mass of 17 amu and hence the observed shift, to higher frequency, is almost the same (80 cm^{-1}).

Table 7 presents the electric response properties computed for the studied benzotriazole derivatives. The dipole moment of 1H-benzotriazole itself is very small; its charge density distribution is polarized in the xy plane (molecular plan) in the x direction. Substitution in the 1-position increases the polarity of the molecule. The effect of electron withdrawing substituents (−Cl) is much greater than that of the electron donating (−OH) one. This is more evident in the case of hyperpolarizability values where the 1-chloro derivative shows a value four times greater than that of the 1-OH derivative. Substitution in the 5-position enhances both the polarity and the polarizibility of the molecule. It is interesting to note that the intrinsic polarizibility $\langle \alpha \rangle$ is almost constant (85 ± 2) for all electron donating substituted benzotriazoles studied (cf. Table 7). Electron withdrawing substituted derivatives of benzotriazole seem to be much more polarized, however. There intrinsic polarizibility $\langle \alpha \rangle$, is not constant and increases as the electron withdrawing effect of the substituent increases.

Conclusions

In this work, we report high resolution FTIR spectra of triazoles and benzotriazoles measured in the solide state as KBr pellets. The predicted vibrational spectrum of 1H-, 2H-1,2,3- and 1,2,4–triazoles and benzotriazoles using a scaling factor of 0.965, are in satisfactory agreement with experiment. It should be emphasized that solid state effects (intermolecular hydrogen bonding) and also a harmonicity of vibrations may cause some differences between the theoretical and experimental spectra. Nevertheless, comparison of the results obtained for the marker bands at the DFT/B3LYP/6-311++G** level of theory; show a very good overall agreement with experiment. Inspection and analysis of the Laplacian of the electron density,$\nabla^2\rho(r)$, reveal that 1,2,3- and 1,2,4-triazoles show completely different topological features for the distribution of the electron density. Thus, while the 1,2,3-isomer is a much more polar molecule; the 1,2,4-isomer is much more polarizable. Bonding characteristics show also different features. This would thus underlie the different features of their vibrational spectra. On the other hand, analysis of $\nabla^2\rho(r)$ for 1H-and 2H-benzotriazoles and comparison of the computed electric response properties reveal very similar topology for the distribution of their electron density. This would thus, underlie the similarity of the corresponding vibrational spectra and substituent effects.

Acknowledgment This work was funded by the Deanship of Scientific Research (DSR) King Abdulaziz University, Jeddah, under grant no. (503-130-1433). The authors acknowledge with thanks DSR support for Scientific Research.

References

1. Wong MW, Leungtoung R, Wentrup C (1993) J Am Chem Soc 115: 2465–2472
2. Nelson DL, Cox MM (2004) Lehninger principles of biochemistry. Freeman, San Francisco
3. Brooks GT, Roberts T (1999) Pesticide chemistry and biosciences: the food-environment challenge. Royal Society of Chemistry, Cambridge
4. Davarski KA, Khalachev NK, Yankova RZ, Raikov S (1998) Chem Heterocycl Compd 34:568–574
5. Kharb RM, Yar S, Sharma PC (2011) Curr Med Chem 18:3265–3297
6. Balabin RM, Safieva RZ (2007) J Near Infrared Spectrosc 15:343–349
7. Zhou CH, Wang Y (2012) Curr Med Chem 19:239–280
8. Balabin RM, Syunyaev RZ (2008) J Colloid Interface Sci 318:167–174
9. Katritzky AR, Rees CW (1984) Comprehensive heterocyclic chemistry. Pergamon, Oxford
10. Gilchrist TL, Gymer GE (1974) Adv Heterocycl Chem 16:33–85
11. Santana L, Teijeira M, Uriarte E, Teran C, Andrei G, Snoeck R, Balzarini J, De CE (1999) Nucleosides Nucleotides 18:733–741
12. Agarwal S, Pande A, Saxena VK, Chowdhury SR (1988) Pol J Pharmacol Pharm 40(3):313–319
13. Cooper K, Steele J, Richardson K. EP 329357. (Chem. Abstr. 1990, 112, 76957u)
14. Oziminskia WP, Dobrowolskia JC, Mazurek AP (2003) J Mol Struct 697:651–653
15. Bugalho SCS, Macoas EMS, Cristiano MLS, Fausto R (2001) Phys Chem Chem Phys 3:3541–3547
16. KonoPski L, Kielczewska A, Maslosz J (1996) Spectrosc Lett 29(1): 143–149
17. Hong W, Clemens B, Gaby P, Jakob W (2000) J Am Chem Soc 122(24):5849–5855
18. Alan RK, Subbu P, Wei-Qiang F (1990) J Chem Soc Perkin Trans 2: 2059–2062
19. Katritzky AR, Yannakopoulou K (1989) Heterocycles 28:1121–1134
20. Abbé GL, Delbeke P, VanEssche G, Leuyten I, VerCanteren K, Toppet S (1990) Bull Soc Chim Belg 99:1007
21. Faure R, Vincent EJ, Elguero J (1983) Heterocycles 20:1713–1716
22. Alan RK, Malhotra N, Wei-Qiang F, Ernst A (1991) J Chem Soc Perkin Trans 2:1545–1547
23. Palmer MH, Kurshid MMP, Rayner TJ, Smith J (1994) Chem Phys 182:27–37
24. Mo O, de Paz JLG, Yanez M (1981) J Phys Chem 90:5597–5604
25. Palmer MH, Simpson I, Wheeler JR (1981) Z Naturforsch 36A: 1246–1252
26. Bergtrup CJ, Nielsen L, Nygaard S, Samdal CE, Sjoergen GO, Soerensen (1988) Acta Chem Scand A 42:500–514
27. Törnkvist C, Bergman J, Liedberg B (1991) J Phys Chem 95:3123–3128
28. Sushko NI, Matveeva NA et al (1990) Zh Prikl Spektrosk 53:323–327
29. Billes F, Endrédi H, Keresztury G (2000) J Mol Struct (Theochem) 530:183–200
30. Bader RFW (1990) Atoms in molecules: a quantum theory. Oxford University Press, Oxford
31. Frisch MJ, Pople JA et al (2009) GAUSSIAN 09, revision a.6. Gaussian Inc, Pittsburgh
32. Becke AD (1993) J Chem Phys 98:5648–5652

33. Burke K, Perdew JP, Wan Y, Dobson JF, Vignale G, Das MP (eds) (1998) Electronic density functional theory: recent progress and new directions. Plenum Press, New York
34. Perdew JP, Burke K, Wang Y (1996) Phys Rev B54:16533–16539
35. Krishnan R, Binkley JS, Seeger R, Pople JA (1980) J Chem Phys 72: 650–655
36. Clark T, Chandrasekhar J, Spitznagel GW, Schrelyer PVR (1983) J Comput Chem 4:294–301
37. AIMAll (Version 13.05.06), Todd A. Keith, TK Gristmill Software, Overland Park KS, USA, 2013 (aim.tkgristmill.com)
38. Kudchadker SA, Rao CNR (1973) Indian J Chem 11:140–142
39. Törnkvist C, Bergman J, Liedberg B (1991) J Phys Chem 95:3123–3128
40. Choi U-S, Tae-W K, Seung-W J, Cheol-J K (1998) Bull Korean Chem Soc 19(3):299–307
41. Buckingham AD (1978) In: Pullman B (ed) Intermolecular interactions: from diatomic to biopolymers. Wiley, Chichester, p 1
42. Kielich S (1977) Molekularna optyka nieliniowa (nonlinear molecular optics). Naukowe, Warsaw
43. Hohm U (2000) Vacuum 58:117–134
44. Schweitzer RC, Morris JB (2000) J Chem Inf Comput Sci 40:1253–1261
45. Gad F, Xiaolin C, Robin L (1996) Chem Phys Lett 29:689–698
46. Wolfgang R, Christoph J, Arnim W, Michael S (1998) J Phys Chem A 102:3048–3059